

Lower critical fields in an ellipsoid-shaped $\text{YBa}_2\text{Cu}_3\text{O}_{6.95}$ single crystal

Ruixing Liang, P. Dosanjh, D. A. Bonn, and W. N. Hardy

Department of Physics, University of British Columbia, Vancouver, British Columbia, Canada V6T 1Z1

A. J. Berlinsky

Department of Physics and Astronomy, McMaster University, Hamilton, Ontario, Canada L8S 4M1

(Received 18 April 1994)

The lower critical fields of $\text{YBa}_2\text{Cu}_3\text{O}_{6.95}$ have been determined by magnetization $M(H)$ measurements using an ellipsoidal-shaped crystal and a thin platelet for $\mathbf{H}\parallel c$ and $\mathbf{H}\perp c$, respectively. Careful data analysis rules out the effects of surface barriers. The data show a linear temperature dependence of H_{c1} below about $0.5T_c$, with $H_{c1}(0)=1100$ Oe and 200 Oe for $\mathbf{H}\parallel c$ and $\mathbf{H}\perp c$, respectively. The anisotropy factor γ is almost temperature independent and has the value 5.6 ± 0.3 . By comparison of the H_{c1} data to results of London penetration-depth measurements, the vortex core energy is found to be linear with temperature.

The value and temperature dependence of the lower critical field H_{c1} of high- T_c superconductors have special importance in superconductivity theories. H_{c1} is proportional to \mathcal{E}_1 ($H_{c1}=4\pi\mathcal{E}_1/\Phi_0$), where \mathcal{E}_1 is the free energy per unit length of an isolated vortex and depends on the current distribution around the vortex, and hence on the penetration depth and on the core energy, i.e., the free-energy cost of the reduction of the order parameter in the core.¹ In spite of numerous studies, the experimental results for H_{c1} are still very confused. For $\text{YBa}_2\text{Cu}_3\text{O}_{7-x}$, the reported low-temperature H_{c1} values range from 400 to 8000 Oe and from 70 to 600 Oe for the field parallel and perpendicular to the c axis, respectively.²⁻⁹ The temperature dependence below $0.5T_c$ is even more controversial: some results show a conventional saturation behavior^{6,8} while others show an unusual upturn at lower temperatures.^{3,5} A linear temperature dependence has also been reported.⁷

The lower critical field H_{c1} marks the onset of the mixed state and has been conventionally determined by measuring the field at which the first Abrikosov vortex penetrates. However, due to the strong bulk pinning in high- T_c superconductors, vortex lines penetrate into the sample very reluctantly and this makes the determination of H_{c1} difficult. The problem is worse if the sample has an imperfect demagnetization geometry (i.e., nonellipsoidal shape), for then vortex penetration starts at sharp corners and edges at an even lower field than H_{c1} , and so broadens out the true H_{c1} point. Nevertheless, until now determinations of H_{c1} for $\text{YBa}_2\text{Cu}_3\text{O}_{7-x}$ have been done on slab-shaped samples with sharp corners and edges. In addition, the Bean-Livingston (BL) surface barrier¹⁰ may push the first penetration field to a value much higher than H_{c1} .¹¹ The combination of the surface barrier and the effects of sharp corners and edges very likely explains the large discrepancies among previous results.

In this paper, we report H_{c1} data on an ellipsoid-shaped high-quality $\text{YBa}_2\text{Cu}_3\text{O}_{6.95}$ single crystal, determined by magnetization $M(H)$ measurements. The

$M(H)$ data were analyzed by the extended Bean critical-state models, both excluding and including the BL surface barrier. We show that the results are not affected by the surface barrier and are therefore a reliable measure of $H_{c1}(T)$.

High-quality $\text{YBa}_2\text{Cu}_3\text{O}_{6.95}$ single crystals were grown by a CuO-BaO flux method using zirconia crucibles as reported elsewhere.¹² We used two crystals. One was polished using $1\ \mu\text{m}$ alumina powder and n -heptane into a nearly ellipsoidal shape with the shortest axis 0.61 mm along the c axis, as shown in Fig. 1, and was free of visible cracks under a scanning electron microscope (SEM). The surface roughness was on the submicrometer scale. After polishing, the crystal was annealed at 860°C for 48 h and then reoxygenated at 450°C for 1 week. The other crystal was a thin plate $1.5\times 0.4\times 0.075\ \text{mm}^3$ with the shortest dimension along the c axis. The two crystals



FIG. 1. SEM surface picture of the ellipsoidal crystal showing submicrometer-order surface roughness. The inset is a photograph of the ellipsoidal crystal with the shortest axis (0.61 mm) along the c axis and the longer axis (0.69 mm) in the ab plane. The crystal was deliberately left with small residual flat regions for purposes of orientation.

came from the same growth batch and were always annealed together. They had the same $T_c = 93.05$ K and $\Delta T_c \approx 0.3$ K, as determined by field-cooling magnetization measurement at 2 Oe. The ellipsoidal crystal, used for $\mathbf{H} \parallel c$ measurements, had a measured demagnetization factor $n = 0.345 \pm 0.005$ (the calculated n value was 0.347), whereas the thin plate used for $\mathbf{H} \perp c$ had $n \approx 0.026$.

The crystals were first cooled in zero field to a chosen temperature, and then the magnetization $M(H)$ was measured with increasing H using a superconducting quantum interference device (SQUID) magnetometer. The shift from perfect shielding, $\delta M(H)$, was then calculated by subtracting the straight-line fit to the low-field part of $M(H)$ from the raw $M(H)$ data. For all temperatures other than the lowest (10 K), the data are well described by the Bean critical-state model without surface barrier. In particular, for $T \geq 20$ K the data have almost no rounding near the first penetration field H_p , which can be determined simply by eye, without using extrapolation techniques commonly used in previous experiments.⁴⁻⁹ The 20-K data ($\mathbf{H} \parallel c$) are shown in the inset to Fig. 2; H_p is increasingly better defined at higher T .

The 10-K data point requires closer scrutiny. According to the Bean critical-state model¹³ for type-II hard superconductors,^{7,14} δM is essentially zero below H_{c1} and

$$4\pi\delta M = A(H - H_{c1})^2/H^* \quad (H_{c1} < H \ll H^*), \quad (1)$$

where A is a constant related to the shape of the sample and H^* a parameter proportional to the critical current density J_c . For this work, the maximum field used was estimated to be less than one-tenth of H^* . However, a plot of $(\delta M)^{1/2}$ vs H for $\mathbf{H} \parallel c$ at 10 K (Fig. 2) shows not

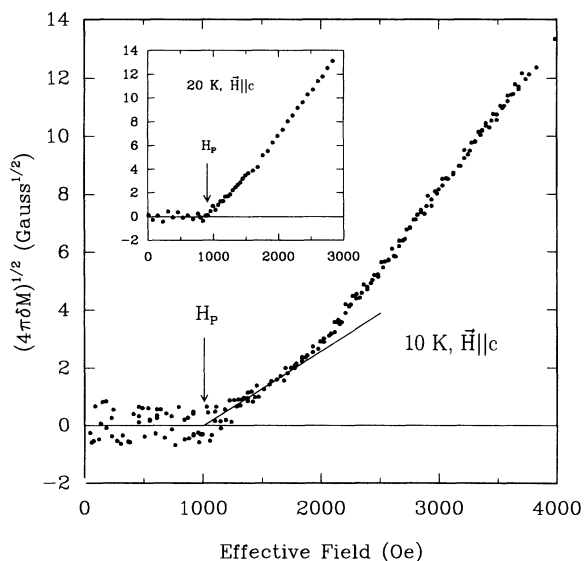


FIG. 2. Plots of $(4\pi\delta M)^{1/2}$ vs H for the ellipsoidal crystal with $\mathbf{H} \parallel c$ at 10 K and 20 K (inset). At 10 K, above the first penetration field H_p , $(4\pi\delta M)^{1/2}$ first increases slowly and then more sharply. The initial slow increase is attributed to the existence of a surface barrier. At 20 K, $(4\pi\delta M)^{1/2}$ is almost linear in H above H_p , consistent with the prediction of the Bean critical-state model without the surface barrier.

a single straight line but a region of slow penetration followed by a more rapid increase with H . Similar behavior has been reported by Naito *et al.*¹⁴ for $(La_{1-x}Sr_x)_2CuO_4$ samples and they explained the initially slow increase of δM as the vortex penetration into sharp corners and edges. Such edges and corners are not present in our case, and we believe that we are starting to see the effect of surface barriers (i.e., J_c is larger near the surface than inside). δM first increases slowly because of the existence of the surface barrier and then increases rapidly when the surface barrier is diminished by the applied field. Therefore, H_{c1} is equal to or lower than H_p , the threshold of the lower straight line, rather than the higher threshold field obtained commonly by extrapolating down from higher fields.

The question is, if there exists a surface barrier, can we still take H_{c1} as the first penetration field H_p or not? The BL surface barrier pushes H_p from H_{c1} to $H_c/\sqrt{2}$ for a perfect surface at 0 K,¹⁰ where H_c is the thermodynamic critical field. In conventional superconductors, experimental observation of the BL surface barrier requires highly polished surfaces because strong local fields caused by the surface roughness destroy the surface barrier and result in $H_p = H_{c1}$. However, in high- T_c superconductors, the Ginzburg-Landau (GL) parameter κ is of order 100, and H_c is so much larger than H_{c1} that local fields may not be strong enough to completely destroy the surface barrier, resulting in $H_c/\sqrt{2} > H_p > H_{c1}$. Burlachkov *et al.*⁸ have included the BL surface barrier in the Bean critical-state model. They supposed that vortices start to penetrate into the sample at distinct points at the surface where the barrier is suppressed by defects such as surface roughness and twin boundaries, and obtained

$$\begin{aligned} \delta M &= C[(1-m)H_{c1}(H - H_{c1})^2/2 + (H - H_{c1})^3/6] \\ &= C\{(H - H_{c1})^2[H - (3m - 2)H_{c1}]\}/6, \end{aligned} \quad (2)$$

where C is a constant related to the shape and critical current density of the sample and m is the ratio of equilibrium magnetization M over the maximum magnetization $M(H_{c1})$. They also estimated $m \approx 0.7$ for $YBa_2Cu_3O_{7-\delta}$ (YBCO) ($\kappa \approx 100$). Putting $m = 0.7$ Eq. (2) yields

$$\delta M \approx C[(H - H_{c1})^2H]/6 \quad (3)$$

or

$$(\delta M/H)^{1/2} \propto H - H_{c1}. \quad (4)$$

This means that a plot of $(\delta M/H)^{1/2}$ vs H gives a straight line with a threshold at H_{c1} . Even in the case where the surface barrier is not completely destroyed but rather just diminished at distinct surface defects so that vortex penetration starts at $H_p > H_{c1}$, Eq. (2) [and so Eq. (4)] still holds in the region somewhat above H_p because the surface barrier diminishes quickly after the first vortex entry. Therefore, H_{c1} can always be obtained by extrapolation of the linear part of the curve to $(\delta M/H)^{1/2} = 0$. In Fig. 3 we have replotted the 10-K data shown in Fig. 2 in the form of $(\delta M/H)^{1/2}$. As is seen, $(\delta M/H)^{1/2}$ is roughly linear with H above H_p , and

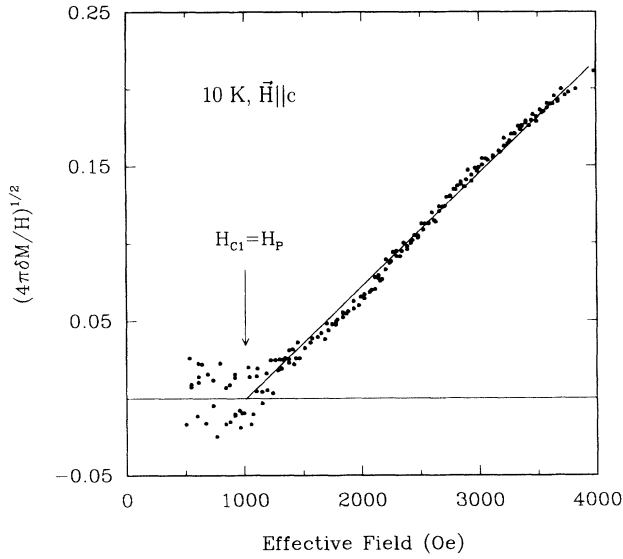


FIG. 3. Plot of $(4\pi\delta M/H)^{1/2}$ vs H replotted from the 10-K data shown in Fig. 2. Above the first penetration field H_p , the data are roughly linear with H and the linear fit gives threshold $H_{c1} = H_p$. This confirms that the surface barrier does not increase H_p beyond H_{c1} .

the linear fit gives $H_{c1} \approx H_p$. This confirms that, in our case, $H_p = H_{c1}$ and the surface barrier does not push H_p higher than H_{c1} but only lowers the rate of vortex entry. Surface roughness of submicrometer order seems to be very effective in destroying the surface barrier. At higher temperature, the surface barrier is further diminished by thermal activation.

The results are summarized in Fig. 4, where we show the temperature dependence of H_{c1} for both $\mathbf{H} \parallel c$ and

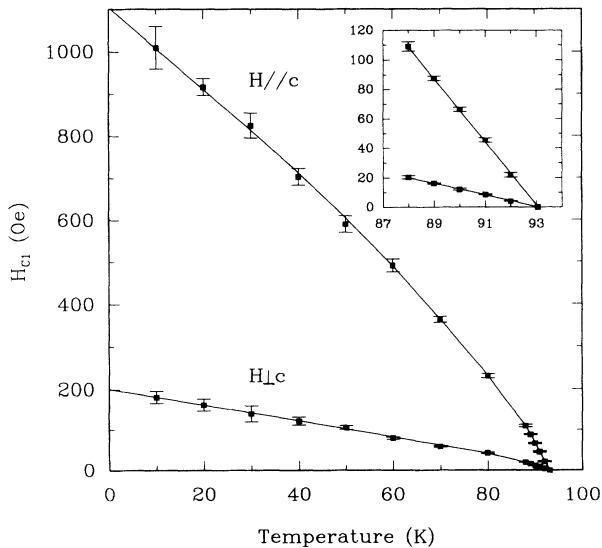


FIG. 4. Lower critical field H_{c1} of $\text{YBa}_2\text{Cu}_3\text{O}_{6.95}$ for both $\mathbf{H} \parallel c$ and $\mathbf{H} \perp c$. The H_{c1} 's are linear with temperature below $0.5T_c$ with slopes of 10.0 ± 0.3 and 1.9 ± 0.1 Oe/K for $\mathbf{H} \parallel c$ and $\mathbf{H} \perp c$, respectively. Extrapolation of the data to zero temperature yields $H_{c1}^{\parallel}(0) = 1100 \pm 50$ Oe and $H_{c1}^{\perp}(0) = 200 \pm 20$ Oe. The inset shows the data near T_c in detail.

$\mathbf{H} \perp c$. At temperatures below $\sim 0.5T_c$, we see neither conventional saturation nor upturn, but essentially a linear temperature dependence with slopes of 10 and 1.9 Oe/K for $\mathbf{H} \parallel c$ and $\mathbf{H} \perp c$, respectively. This is qualitatively different from the saturation at low temperatures expected for a conventional s -wave BCS superconductor¹⁵ and is consistent with an energy gap with line nodes,¹⁶ as predicted by models that lead to d -wave superconductivity.¹⁷ It is worth mentioning that, although the model of quasi-two-dimensional superconducting sheets alternating with normal layers¹⁸ can also explain the lack of the saturation in H_{c1} at low temperatures, it produces a temperature dependent $\gamma = H_{c1}^{\parallel}/H_{c1}^{\perp}$ that is inconsistent with our observations in $\text{YBa}_2\text{Cu}_3\text{O}_{6.95}$. The anisotropy factor γ that we observed is almost temperature independent and has the value 5.6 ± 0.3 , consistent with the values 5–6 estimated for H_{c2} measurements.¹⁹ This is larger than the values 3–4 in previous H_{c1} measurements^{4–7} made on slab-shaped samples with the shortest dimensions along the c axis. Sharp corners and edges in the slab geometry likely lead to underestimation of H_{c1}^{\parallel} and γ . We emphasize that the temperature independence of γ is a strong corroborating evidence that we have measured the true H_{c1} rather than a surface-condition-dependent first entry field, because, first, the surface barriers in the two directions are highly unlikely to be the same, and secondly, the ellipsoid and the thin plate crystal have completely different surface roughnesses.

The experimental value for H_{c1} is surprisingly large compared to what one might expect from Ginzburg-Landau theory. In general, the vortex line energy, $\mathcal{E}_1 = \Phi_0 H_{c1} / (4\pi)$ is a sum of two parts,¹

$$\mathcal{E}_1 = E_{\text{em}} + E_{\text{core}}, \quad (5)$$

where, for a large- κ material,

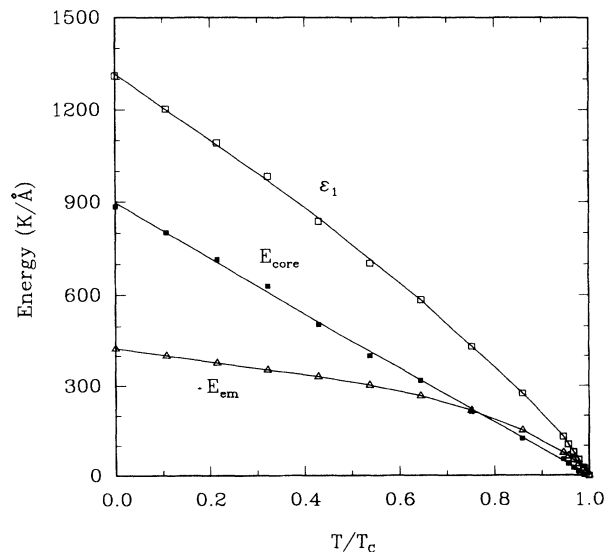


FIG. 5. Total line energy \mathcal{E}_1 , electromagnetic energy E_{em} , and core energy E_{core} of a vortex line. E_{core} is found to be linear with temperature all the way from $T=0$ to T_c .

$$E_{\text{em}} = \left[\frac{\Phi_0}{4\pi\lambda} \right]^2 \ln\kappa \quad (6)$$

is the energy of the magnetic field and of the supercurrent associated with the vortex. In GL theory for an s -wave superconductor,²¹ the effect of the core energy is to add a term of order 0.5 to $\ln\kappa$, which is negligible if κ is large, as it is for YBCO ($\kappa \approx 70$). Assigning all of the vortex energy to E_{em} and using $H_{c1}^{\parallel}(0) = 1100$ Oe implies $\lambda_{ab}(0) \approx 800$ Å, in serious disagreement with the value of 1400 Å by μ SR and infrared measurements.^{22,23} This comparison suggests that the core energy of an isolated vortex in YBa₂Cu₃O_{6.95} is substantially larger than one would expect for a conventional superconductor. In fact, using the value of $\lambda_{ab}(0) \approx 1400$ Å from muon spin resonance (μ SR)²² and infrared²³ measurements and $\Delta\lambda_{ab}(T)$ from microwave measurement²⁰ allows us to determine E_{em} and hence to extract the core energy E_{core} , over the entire temperature range $0 < T < T_c$. This analysis is shown in Fig. 5, in which \mathcal{E}_1 , E_{em} , and E_{core} are plotted vs T/T_c . The most striking features of this analysis are the near-perfect linearity of E_{core} over the entire temperature range, and the large value of E_{core} , particularly at low T .

We do not claim to understand the origin of this behavior. We simply note that all of our data suggest an

unconventional nature for the superconductivity of YBa₂Cu₃O_{6.95} and that little or nothing is known about the microscopic structure of vortices in such a system. The only relevant results of which we are aware are due to Volovik²⁴ who finds that the density of states at zero energy for a d -wave vortex is enhanced by a factor of κ over that for an s -wave vortex. Clearly, further theoretical work on this subject is needed.

In conclusion we have measured the lower critical field H_{c1} of YBa₂Cu₃O_{6.95} using an ellipsoid-shaped crystal (thin-plate crystal for H perpendicular to the c axis) and found a linear temperature dependence of H_{c1} below $0.5T_c$. This is very different from that expected for conventional superconductivity but is consistent with that expected for a pairing state with line nodes in the gap. Combined with $\Delta\lambda_{ab}(T)$ data²⁰ and values of $\lambda_{ab}(0)$ from infrared²³ and μ SR measurements,²² our results suggest that the vortex core energy is proportional to $1 - T/T_c$ over the entire temperature range.

The authors would like to thank Dr. J. F. Carolan, Dr. C. Kallin, and Dr. P. Soininen for very valuable discussions. This work was supported by the Natural Science and Engineering Research Council of Canada and the Canadian Institute for Advanced Research.

¹M. Tinkham, *Introduction to Superconductivity* (McGraw-Hill, New York, 1975), Chap. 5.

²A. Umezawa, G. W. Crabtree, J. Z. Liu, T. J. Moran, S. K. Malik, L. H. Nunez, W. L. Kwok, and C. H. Sowers, *Phys. Rev. B* **38**, 2843 (1988).

³J. P. Ströbel, A. Thomä, B. Hensel, H. Adrian, and G. Saemann-Ischenko, *Physica C* **153-155**, 1537 (1988); H. Adrian, W. Assmus, A. Höhr, J. Kowalewski, H. Spille, and F. Steglich, *ibid.* **162-164**, 329 (1989); A. Umezawa, G. W. Crabtree, K. G. Vandervoort, U. Welp, W. K. Kwok, and J. Z. Liu, *ibid.* **163-164**, 733 (1989); T. Ishii and T. Yamada, *ibid.* **159**, 483 (1989).

⁴Y. Yeshurun, A. P. Malozemoff, F. Holtzberg, and T. R. Dinger, *Phys. Rev. B* **38**, 11 828 (1988); L. Krusin-Elbaum, A. P. Malozemoff, Y. Yeshurun, D. C. Cronemeyer, and F. Holtzberg, *ibid.* **39**, 2936 (1989).

⁵M. W. McElfresh, Y. Yeshurun, A. P. Malozemoff, and F. Holtzberg, *Physica A* **168**, 308 (1990).

⁶Dong-Ho Wu and S. Sridhar, *Phys. Rev. Lett.* **65**, 2074 (1990).

⁷V. V. Moshchalkov, J. Y. Henry, C. Marin, J. Rossat-Mignod, and J. F. Jachou, *Physica C* **175**, 407 (1991).

⁸L. Burlachkov, Y. Yeshurun, M. Konczykowski, and F. Holtzberg, *Phys. Rev. B* **45**, 8193 (1992).

⁹D.-X. Chen, R. B. Goldfarb, R. W. Cross, and A. Sanchez, *Phys. Rev. B* **48**, 6426 (1993).

¹⁰C. P. Bean and J. B. Livingston, *Phys. Rev. Lett.* **12**, 14 (1964).

¹¹M. Konczykowski, L. I. Burlachkov, Y. Yeshurun, and F. Holtzberg, *Phys. Rev. B* **43**, 13 707 (1991).

¹²Ruixing Liang, P. Dosanjh, D. A. Bonn, D. J. Baar, J. F. Carolan, and W. N. Hardy, *Physica C* **195**, 51 (1992).

¹³C. P. Bean, *Rev. Mod. Phys.* **36**, 31 (1964).

¹⁴M. Naito, A. Matsuda, K. Kitazawa, S. Kambe, I. Tanaka, and H. Kojima, *Phys. Rev. B* **41**, 4823 (1990).

¹⁵B. Muhlschlegel, *Z. Phys.* **155**, 313 (1959).

¹⁶James Annett, Nigel Goldenfeld, and S. R. Renn, *Phys. Rev. B* **43**, 2778 (1991).

¹⁷D. J. Scalapino, E. Loh, and J. Hirsch, *Phys. Rev. B* **34**, 8190 (1986); N. E. Bickers, D. J. Scalapino, and R. T. Scalettar, *Int. J. Mod. Phys. B* **1**, 687 (1987); P. Monthoux, A. V. Balatsky, and D. Pines, *Phys. Rev. Lett.* **67**, 3448 (1991).

¹⁸T. Koyama, N. Takezawa, and M. Tachiki, *Physica C* **168**, 69 (1990).

¹⁹U. Welp, W. K. Kwok, G. W. Crabtree, K. G. Vandervoort, and J. Z. Liu, *Phys. Rev. Lett.* **62**, 1908 (1989); Z. D. Hao, J. R. Clem, M. W. McElfresh, L. Civale, A. P. Malozemoff, and F. Holtzberg, *Phys. Rev. B* **43**, 2844 (1991); Y. X. Jia, J. Z. Liu, M. D. Lan, P. Klavins, R. N. Shelton, and H. B. Radousky, *ibid.* **45**, 10 609 (1992).

²⁰W. N. Hardy, D. A. Bonn, D. C. Morgan, Ruixing Liang, and Kuan Zhang, *Phys. Rev. Lett.* **20**, 3999 (1993).

²¹Richard A. Klemm and John R. Clem, *Phys. Rev. B* **21**, 1868 (1980); V. G. Kogan, *ibid.* **24**, 1572 (1981); C.-R. Hu, *ibid.* **6**, 1756 (1972).

²²D. A. Bonn, Ruixing Liang, T. M. Riseman, D. J. Baar, D. C. Morgan, Kuan Zhang, P. Dosanjh, T. L. Duty, A. MacFarlane, G. D. Morris, J. H. Drewier, W. N. Hardy, C. Kallin, and A. J. Berlinsky, *Phys. Rev. B* **47**, 11 314 (1993).

²³D. N. Basov, A. V. Puchkov, R. A. Hughes, T. Strach, J. Preston, T. Timusk, D. A. Bonn, R. Liang, and W. N. Hardy, *Phys. Rev. B* **49**, 12 165 (1994).

²⁴G. E. Volovik, *Pis'ma Zh. Eksp. Teor. Fiz.* **58**, 444 (1993) [*JETP Lett.* **58**, 455 (1993)]; **58**, 457 (1993) [**58**, 469 (1993)].

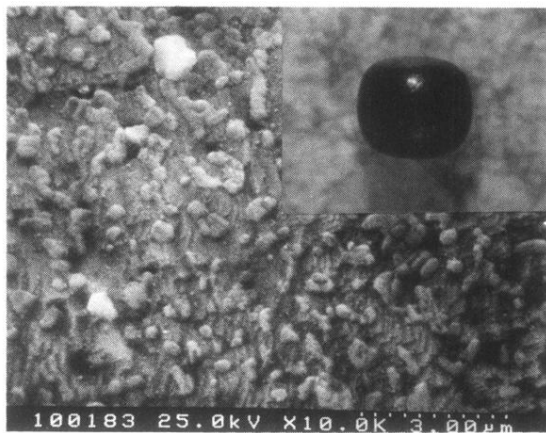


FIG. 1. SEM surface picture of the ellipsoidal crystal showing submicrometer-order surface roughness. The inset is a photograph of the ellipsoidal crystal with the shortest axis (0.61 mm) along the c axis and the longer axis (0.69 nm in the ab plane). The crystal was deliberately left with small residual flat regions for purposes of orientation.